Supporting Information

Detecting patchy nanoparticle assembly at the single-particle level

S. Pothorszky, D. Zámbó, D. Szekrényes, Z. Hajnal, A. Deák*
E-mail: andras.deak@energia.mta.hu

Interaction calculations

The rod was modelled as a two hemisphere-capped cylinder, particle dimensions were obtained from scanning electron microscopy measurements.

Dispersion interaction for the tip and side located nanospheres at a nanorod:[1]

$$U_{disp}^{tip} = \frac{-A}{6\delta} * \frac{a * a_R}{(a + a_R)} \qquad (1)$$

$$U_{disp}^{side} = \frac{-A}{6\delta} * \left(\frac{a_R * a^2}{(a + a_R)}\right)^{1/2} \qquad (2)$$

where a and a_r refer to the sphere and rod radii, respectively. A is the Hamaker-coefficient for the gold-water-gold system (2.5×10^{-19} J)[2] and δ is the surface-to-surface separation between the particles.

For the electric double layer interaction, the following scheme shows the physical dimensions of the particles and the surface charge densities. The surface charge densities of spherical particles were obtained from electrophoretic (zeta-potential) measurements using:[3]

$$\sigma = \frac{\varepsilon\varepsilon_0 k_B T}{ze}\kappa\left[2\sinh\left(\frac{\zeta ze}{2k_BT}\right) + \frac{4}{\kappa a}\tanh\left(\frac{\zeta ze}{4k_BT}\right)\right] \qquad (3)$$

where z is the valence of ions, ζ is the zeta-potential of the particle, e is the elementary charge, ε_0 is the vacuum permittivity and ε is the relative permittivity of water, κ is the Debye parameter and a is the particle radius.

For nanorods, the tip surface charge density was experimentally modelled using a spherical r=32 nm CTAB capped gold nanoparticle (prepared according to Ref. [4]), which was processed with cysteamine is the same manner as the CTAB capped rods during the tip-selective functionalization. To obtain the side-value, the rods were fully PEGylated (without the prior addition of cysteamine) and their electrophoretic mobility measured.

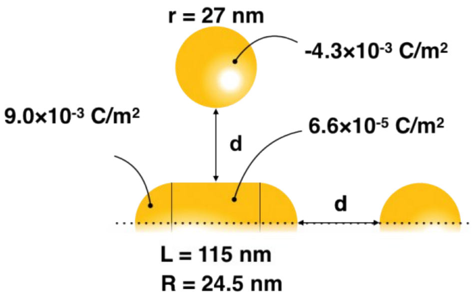

During the finite-element method calculation, the nonlinear Poisson-Boltzmann equation has been solved for the above depicted two geometrical arrangements at different surface-to-surface separation distances (d) in the range of 0.5 - 50 nm, using the “Electrostatics” and “Transport of Diluted Species” modules. From the obtained electric field and ion-concentration distribution, the free-energy of the system was obtained based on Ref. [5]:

$$\Delta G^{EDL} = \int (E \cdot D/2 + \rho^{m}\Phi\ - \Delta\Pi)dv \tag{4}$$

where **E**: local electric field; **D**: local displacement field; ρ_m: local charge density in the aqueous medium; Φ: local electric potential ΔΠ: osmotic contribution[6] of the ion cloud surrounding the particles. The integration is performed over the whole simulation volume (mobile charges and osmotic contribution arising naturally only in the aqueous medium). The simulation volume was a 400 nm high cylindrical volume (400 nm diameter), with the rod positioned in its center along the cylinder axis. FEM (finite element modelling) relies on meshes of the simulation volume, that should adapt to specific properties of the studied systems. In the present case, the tetrahedral mesh elements of the particles and in their vicinity were chosen to be very fine, with average dimensions ~1 nm and maximum diameter of 4 nm. Tetrahedral mesh elements of more remote parts of the aqueous medium were allowed to "grow" up to 40 nm. This is appropriate for regions where ion concentrations do not fluctuate considerably. However, additional 8 (so called boundary) layers of mesh elements with gradually growing thickness from 1 to 2 nm were introduced in the vicinity of the nanoparticle surfaces to allow proper resolution of concentration gradients of the "double layers". The solvent region "connecting" the nanoparticles, was defined as an extra cylindrical volume section, where the mesh was kept consistently as fine as the resolution of the nanoparticle surfaces (max. 4, average ~1 nm). The reference state (ΔG^{EDL}_{0}) was chosen so that the electric double layers did not overlap. This was the case at 100 nm surface-to-surface separation for both the tip and side arrangements. The final free enthalpy change was calculated as $\Delta G^{EDL} - \Delta G^{EDL}_{0}$. At the particle surfaces constant surface charge boundary condition was applied, with values obtained from separate mobility measurements after nanoparticle preparation.

Supporting Figures

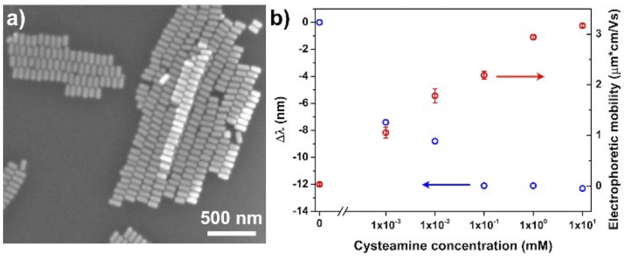

Figure S1 (a) Characteristic SEM image of the as-prepared gold nanorods. (b) Blueshift (left axis) and electrophoretic mobility (right axis) of the patchy particles as a function of cysteamine concentration applied during the ligand replacement.

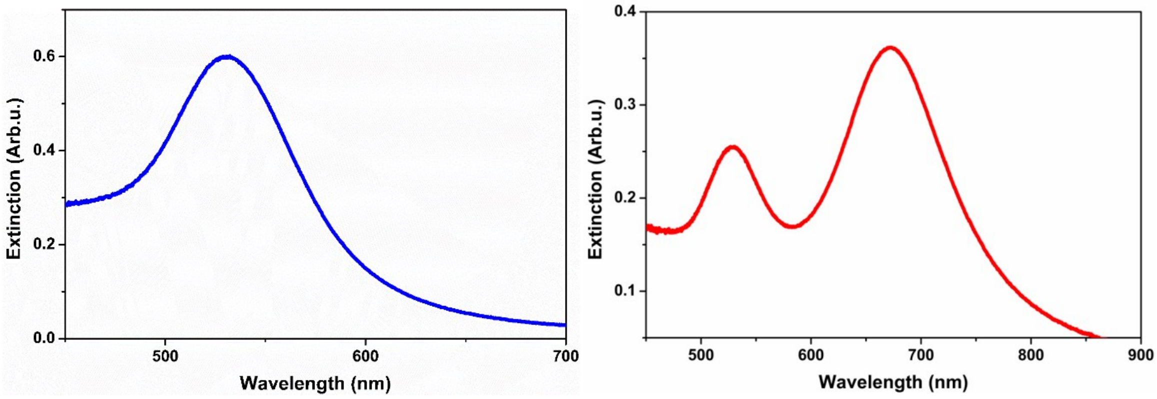

Figure S2: Extinction spectra of the as-prepared gold spheres (left) and rods (right).

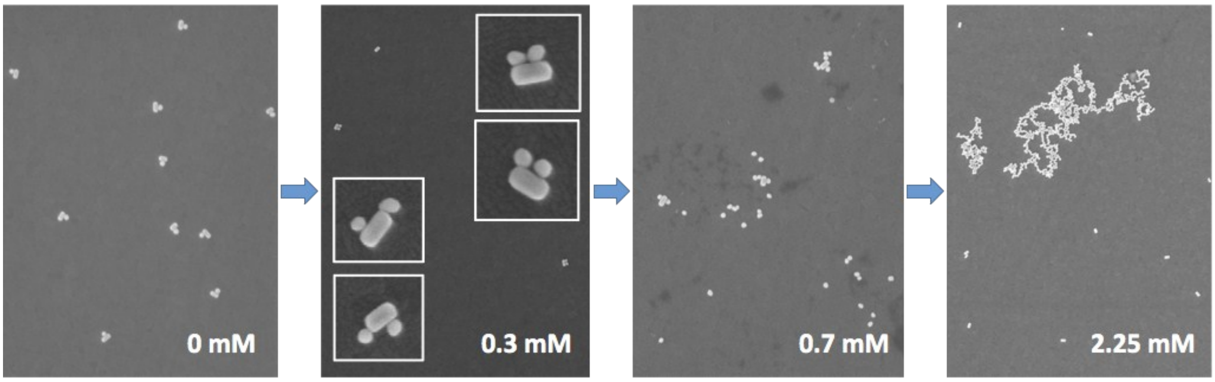

Figure S3: SEM images of the assembled structures obtained at different KCl concentrations.

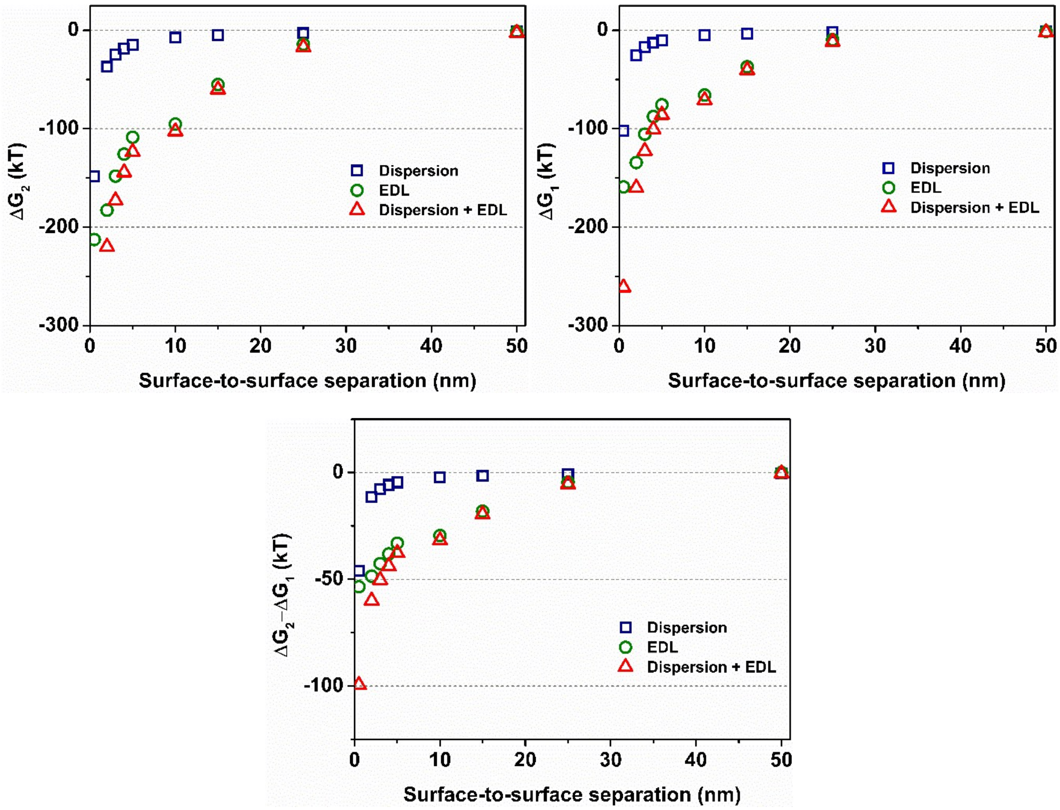

Figure S4: Interaction energies and their difference of the dispersion and electric double layer interaction energies between the side (ΔG_2) and tip (ΔG_1) configurations.

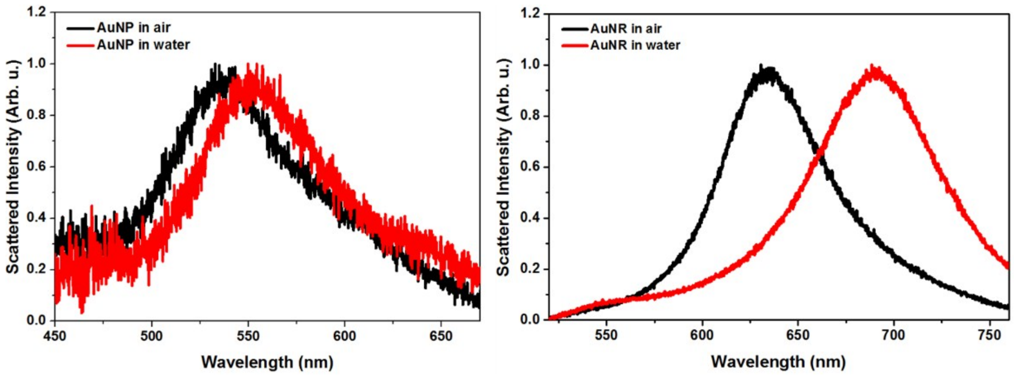

Figure S5: Scattering spectra of a single nanosphere (left) and a nanorod (right) measured in dry (black) and water-filled (red) liquid chamber.

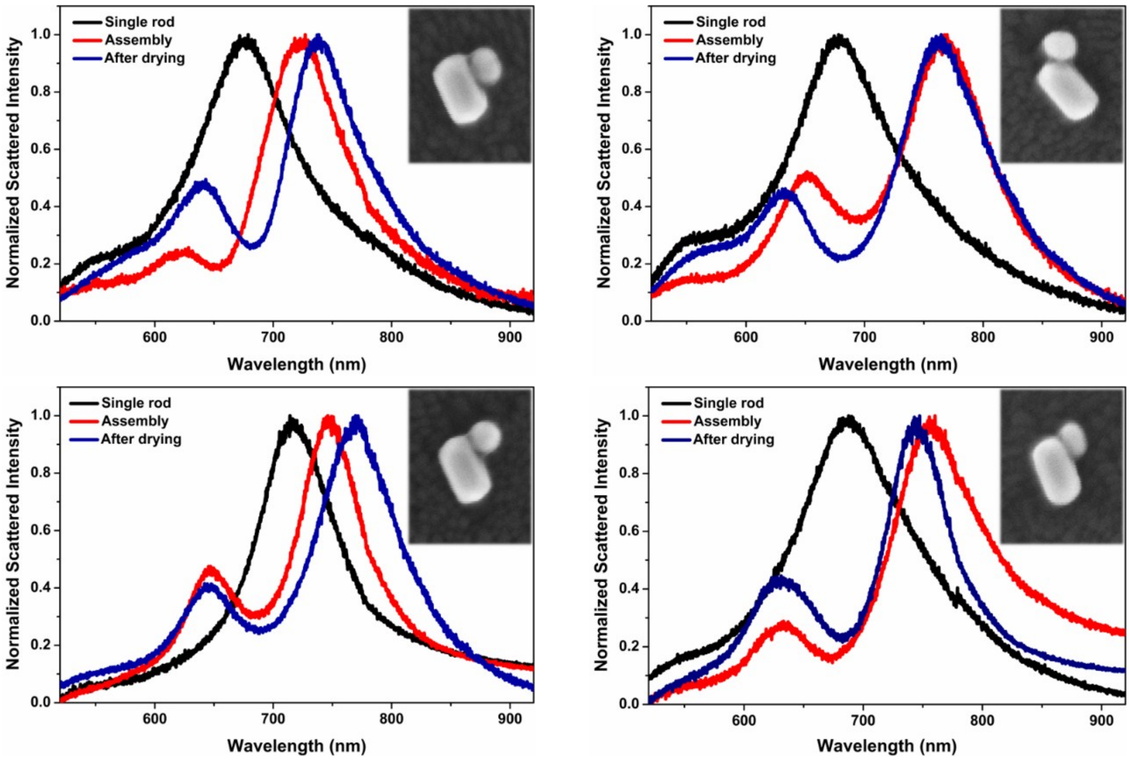

Figure S6: Scattering spectra of the initial nanorod (black), the assembled (red) and the dried (blue) heterodimer. Measurement on the dry sample was performed before the SEM investigation.

References

1 D. A. Walker, C. E. Wilmer, B. Kowalczyk, K. J. M. Bishop and B. A. Grzybowski, *Nano Letters*, 2010, **10**, 2275–2280.
2 S. Biggs and P. Mulvaney, *The Journal of Chemical Physics*, 1994, **100**, 8501–8505.
3 J. N. Israelachvili, *Intermolecular and surface forces*, Academic Press, Burlington, MA, 3rd ed., 2011.
4 N. Pazos-Perez, F. J. Garcia de Abajo, A. Fery and R. A. Alvarez-Puebla, *Langmuir*, 2012, **28**, 8909–8914.
5 K. A. Sharp and B. Honig, *Journal of Physical Chemistry*, 1990, **94**, 7684–7692.
6 P. W. Atkins and J. De Paula, *Physical chemistry*, W.H. Freeman, New York, 9th ed., 2010.